II d 11

AN INVESTIGATION OF STRESS-STRAIN AND STRENGTH CHARACTERISTICS OF COHESIONLESS SOILS BY TRIAXIAL COMPRESSION TESTS

LIANG-SHENG CHEN

Research Fellow in Soil Mechanics
Graduate School of Engineering, Harvard University, Cambridge, Massachusetts, U.S.A.

SYNOPSIS

During 1943 and 1944, the author investigated the stress-strain and strength characteristics of cohesionless soils by means of triaxial compression tests. High accuracy in the determination of the entire stress-strain curve was the principal purpose of this investigation. Among the variables which were investigated are: minor principal stress, density, grain size and shape.

This research was conducted at the Soil Mechanics Laboratory of the Graduate School of Engineering, Harvard University, under the supervision of Professor Arthur Casagrande.

GENERAL DESCRIPTION OF APPARATUS

The apparatus used is shown in Figs. 1 and 2. The following two points are worth noting: (1) The test specimens were cylindrical, enveloped in a thin rubber tube, seated on a metal base and covered by a metal cap. The rubber tube was bound to the base and the cap by means of rubber bands. A hole through the base permitted the evacuation of air from the test specimens. The partial vacuum thus created induced lateral pressure on the test specimens and was measured by a mercury manometer. (2) The loading device consists essentially of a platform scales and a loading yoke. The yoke is operated by means of a mechanical jack and a handwheel not shown in Figs. 1 and 2.

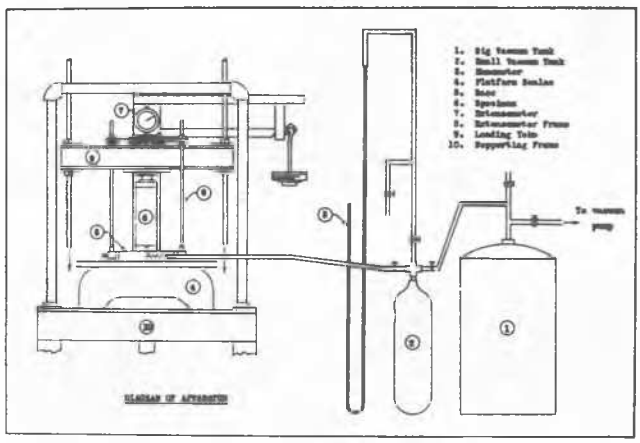

FIG. 1

LOAD TRANSMISSION ARRANGEMENT

The different pieces of equipment used to transmit load from the loading yoke to a test specimen are shown in Fig. 3. A cup was inserted between the cap and the yoke attachment. This cup insures a ring contact between its conical surface and the spherical surface of the yoke attachment. The friction which is mobilized at this contact ring is sufficient to prevent tilting of the cap toward the end of tests. A 3/4" hole at the center of the yoke attachment and the cup enables the stem of an extensometer (Fig. 1) to establish a direct contact with the cap, thus improving the accuracy in the measurement of the axial deformation of test specimens.

EQUIPMENT AND METHOD FOR PLACING AND COMPACTING TEST SPECIMENS.

Fig. 4(a) shows a test specimen being prepared; Fig. 4(b) the various pieces of equipment used for its preparation. Attention is called to the construction of the following items: (1) forming jacket; (2) spoon; (3) tampers.

The forming jacket consists essentially of two half cylinders which are matched by means of dowel pins and are pressed against each other by bolts. To seat the jacket tightly on the base, a rubber gasket was used. The top end of the jacket is reduced in thickness and rounded to permit rolling the open end of the rubber tube over it. An outlet on the side of one half of the jacket, together with a system of longitudinal and circumferential fine grooves on the inside of the jacket, facilitate the evacuation of air from the enclosed space formed by the inside of the jacket, the rubber tube, and the rubber gasket. Evacuation of this space was essential to the preparation of neat test specimens.

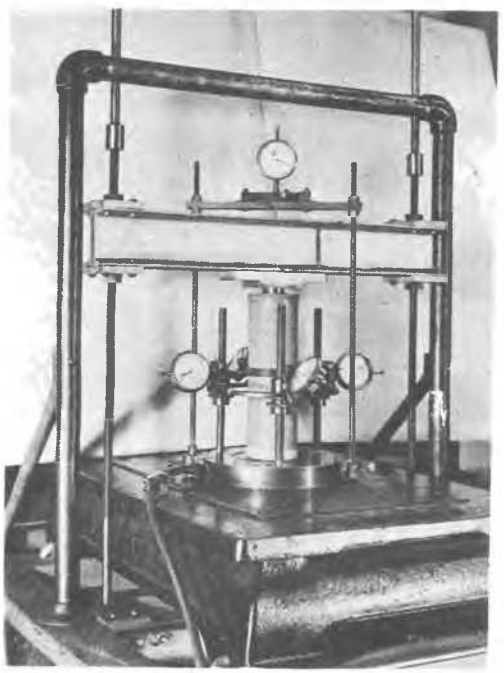

Test in progress

FIG. 2

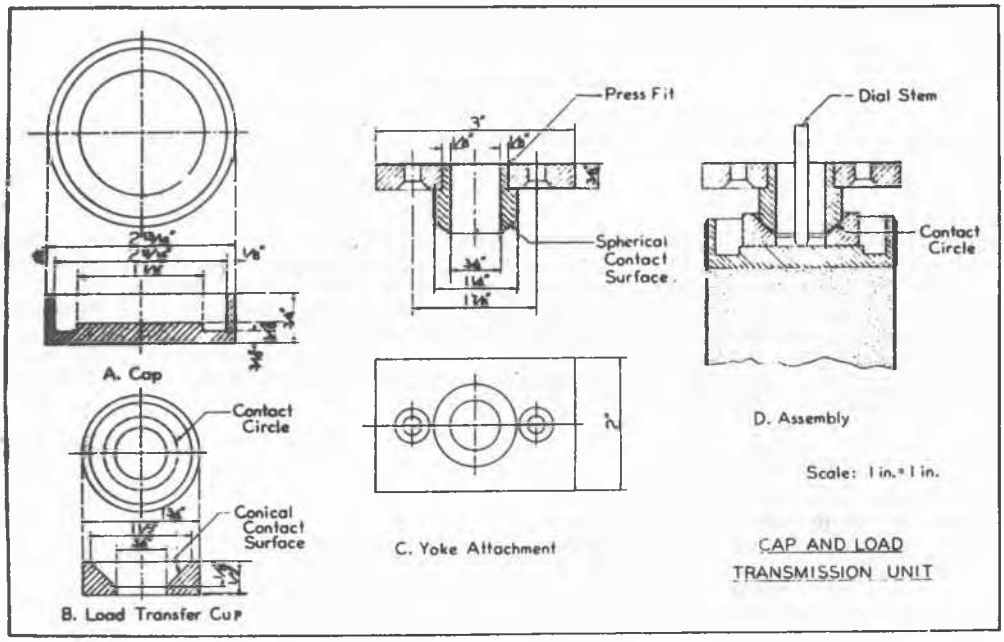

FIG. 3

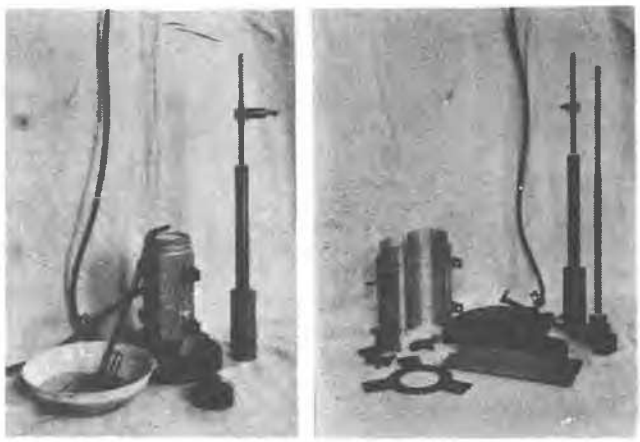

a. Test specimen being prepared

b. Pieces of equipment for preparing test specimen

Preparation of test specimen

FIG. 4

The spoon (Figs. 4 and 5) was given a long handle so that soil could be placed with a minimum drop. A short arm hinged at the top of this handle and a connecting wire permit the dumping of soil in a controlled manner. The importance of control in placing soil in the preparation of loose specimens and in the prevention of segregation of grains of well-graded materials cannot be over-emphasized.

The important feature in the design of the tampers for compacting soil is their two-piece construction which is illustrated in Figs. 4 and 6. During compaction, the anvil rested on top of the soil, while the tamping weight was allowed to fall freely from a predetermined height which was controlled by the position of a movable clamp along the stem of the anvil. Between successive blows, the tamper was moved slightly over the surface of the soil to effect a more uniform compaction. The tamping weight was made slightly smaller in

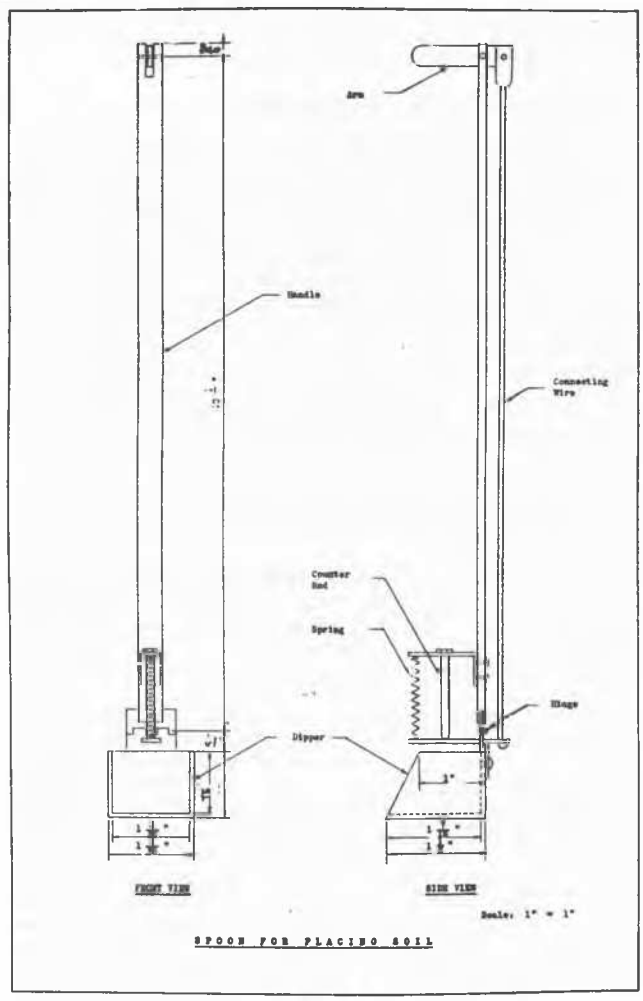

FIG. 5

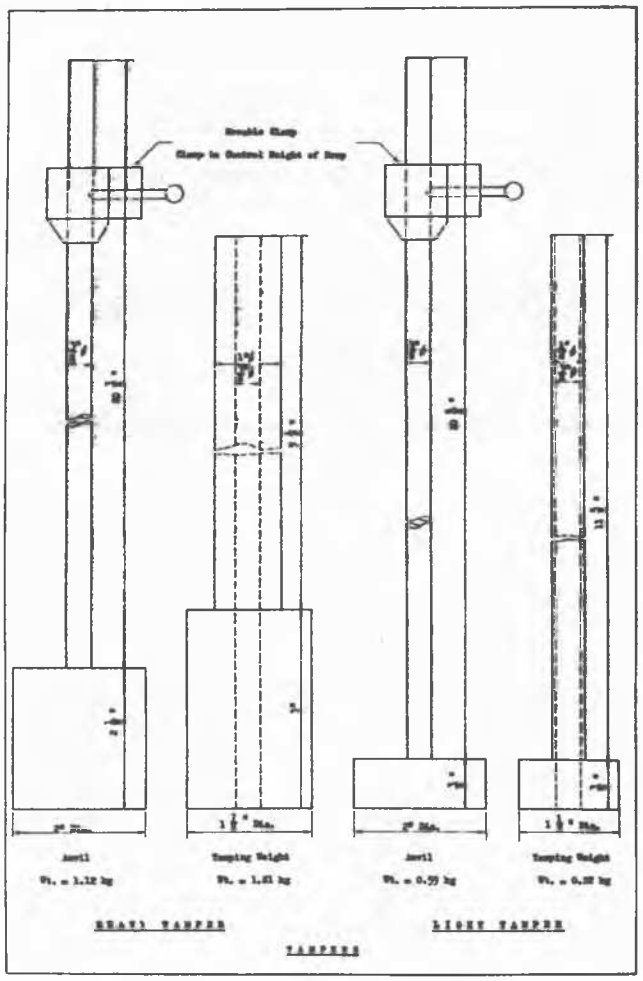

FIG. 6

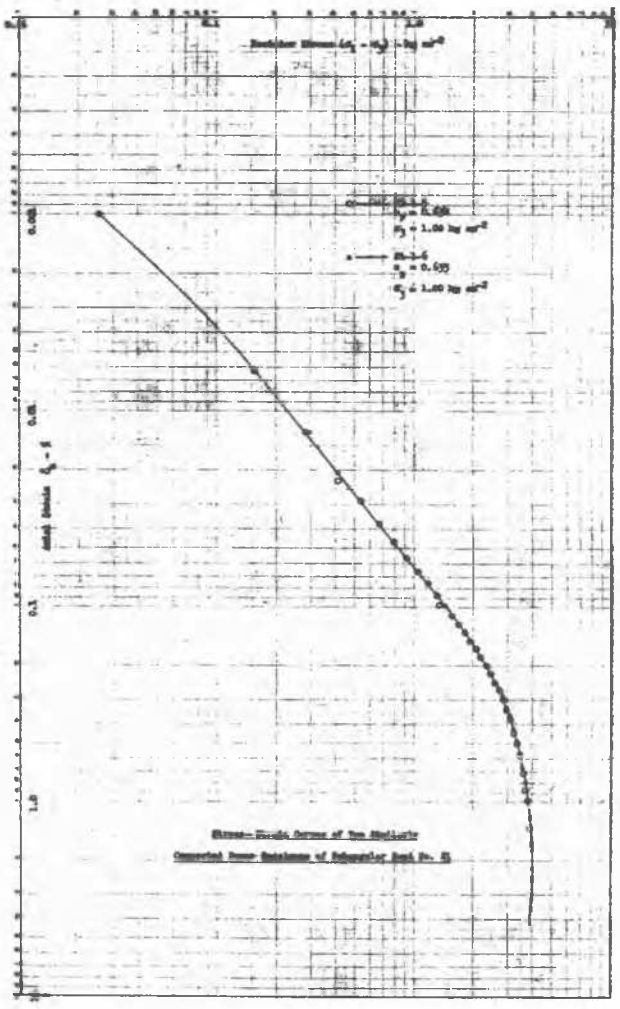

FIG. 7

diameter than the anvil to avoid damaging the rubber tube. To produce a wide range of density, two different tamping weights were used.

The dimensions of all test specimens at the start of the test were: diameter - 2.8 in., height - 7 in. Except for the loosest specimens, all test specimens were compacted in ten layers. An arbitrarily chosen total number of blows by a tamping weight was distributed among the ten layers according to a linear variation; that is, the number of blows given to each layer exceeded that given to the preceding layer by a constant value. The variation was so adjusted that the test specimen, when evacuated and compressed, would deform symmetrically with respect to its midheight, an indication of a uniform density along the height of the test specimen.

TEST PROCEDURE

The loading of a test specimen was done in increments applied at regular time intervals. The axial deformation of the specimen was measured by a dial extensometer (Figs. 1 and 2), whereas its lateral expansion was usually measured by means of a caliper at the midheight cross-section. In a few tests, dial extensometers were used, as shown in Fig. 2, to obtain greater accuracy.

The vacuum inside of a test specimen was kept constant during a test. The lateral pressure on the specimen, however, changed slightly during the test owing to the changing confining pressure exerted by the thin rubber tube as the specimen expanded laterally.

DESCRIPTION OF MATERIALS TESTED

A description of the materials tested is found in Fig. 24. Each tested material was given a number and is designated by that number elsewhere in this paper. All materials tested were air-dried.

GRAPHICAL PRESENTATION OF STRESS-DEFORMATION RELATIONSHIPS.

Figs. 7 through 9 serve to illustrate the method of presenting stress-deformation relationships. Figs. 7 and 8 show the stress-strain curves of two similarly compacted dense specimens of subangular sand No. 81 (see Fig. 24), on logarithmic and arithmetic plots respectively. In each figure, the abscissa represents the deviator stress (i.e. the difference between the major principal or axial stress and the minor principal or lateral stress) at the midheight cross-section of the test specimen; the ordinate represents the axial strain (that is, the ratio of the compression of a test specimen to its height at the start of loading). Comparison of Figs. 7 and 8 shows that a logarithmic plot presents the first portion of a stress-strain curve more accurately than an arithmetic plot. This advantage of a loga-

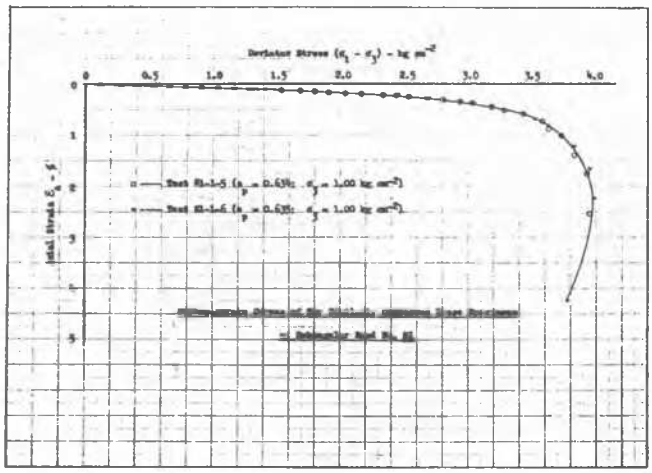

FIG. 8

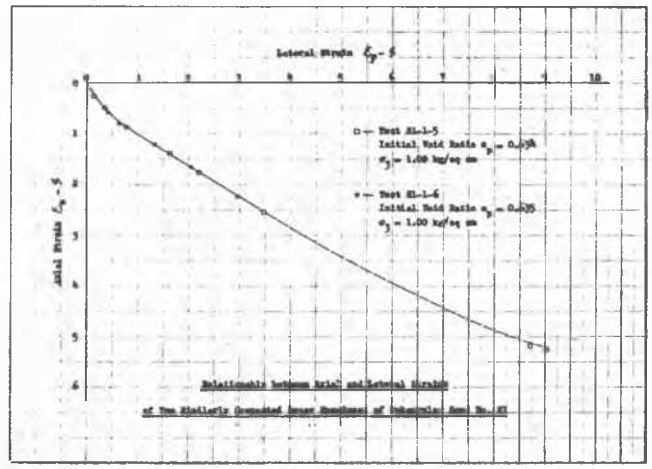

FIG. 9

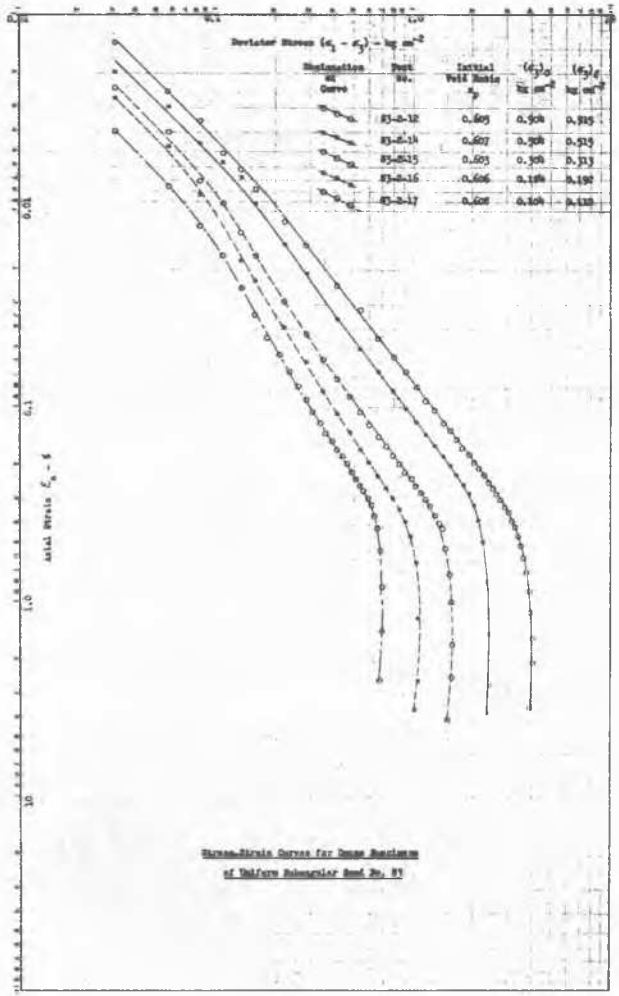

FIG. 10

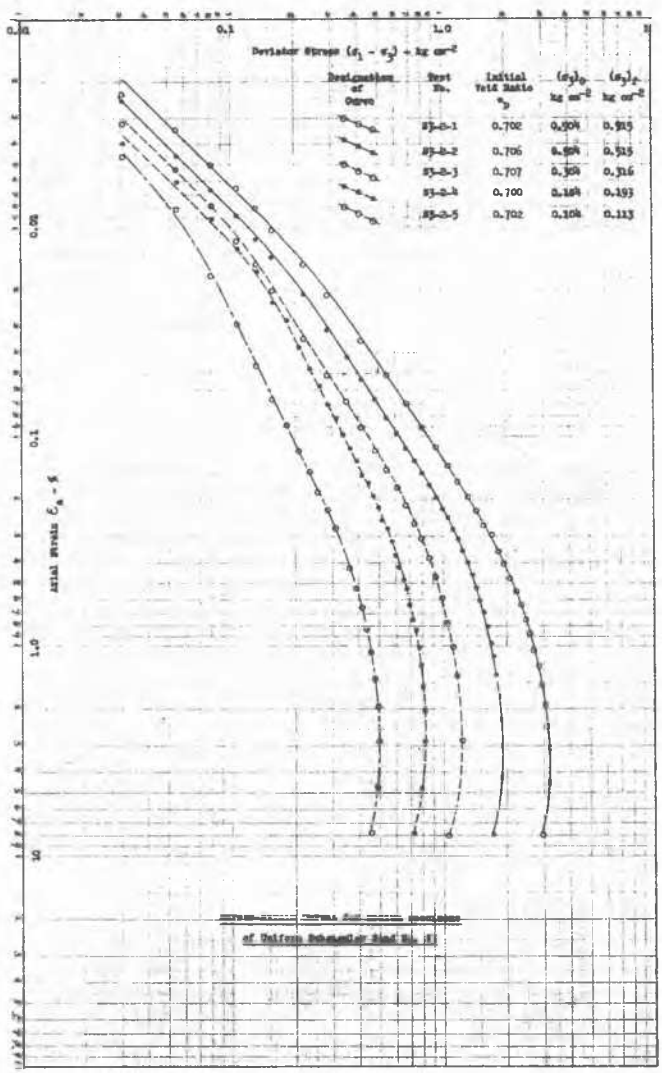

FIG. 11

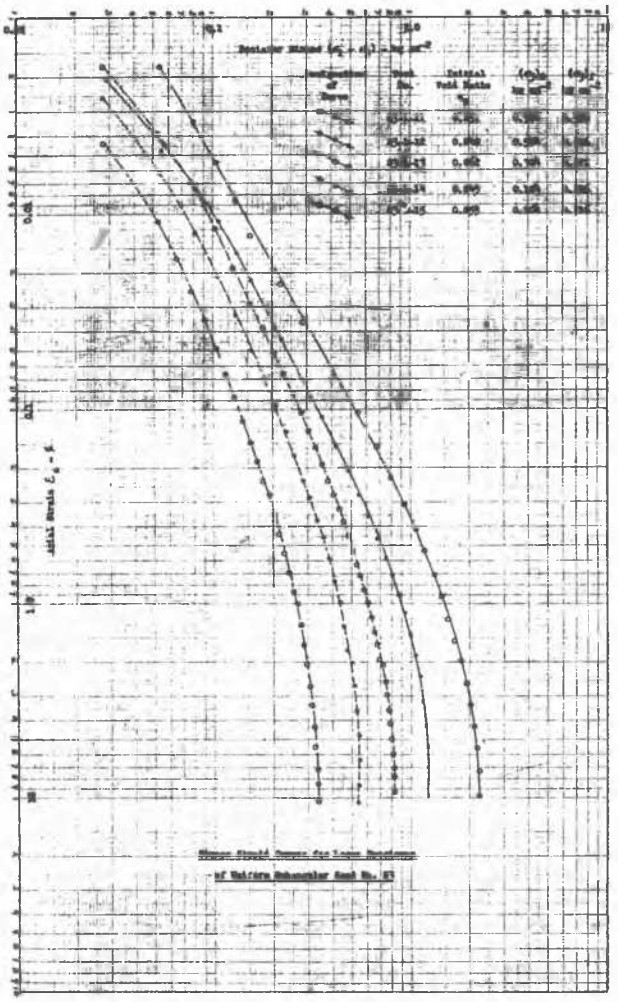

FIG.12

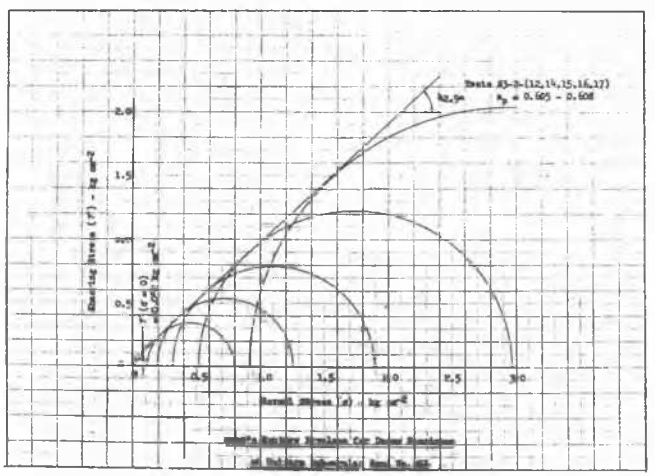

FIG.13

rithmic plot becomes more apparent when a group of stress-strain curves are plotted and compared on one sheet.

Fig. 9 shows the relationship between the lateral and axial strains of the two specimens mentioned above. The lateral strain is defined as the ratio of the increase in the diameter at the midheight cross-section to that diameter at the start of the test.

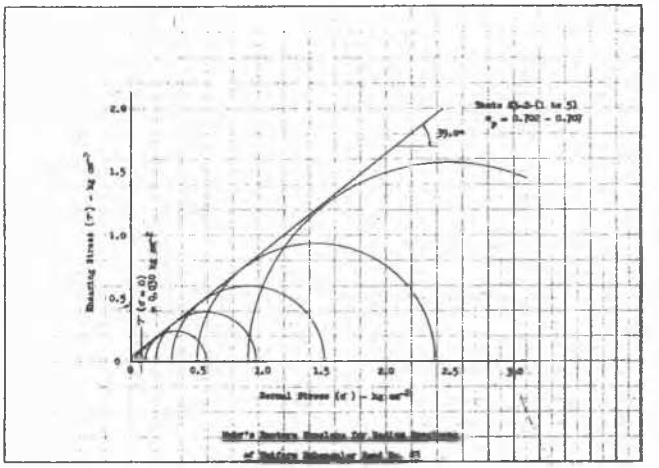

FIG.14

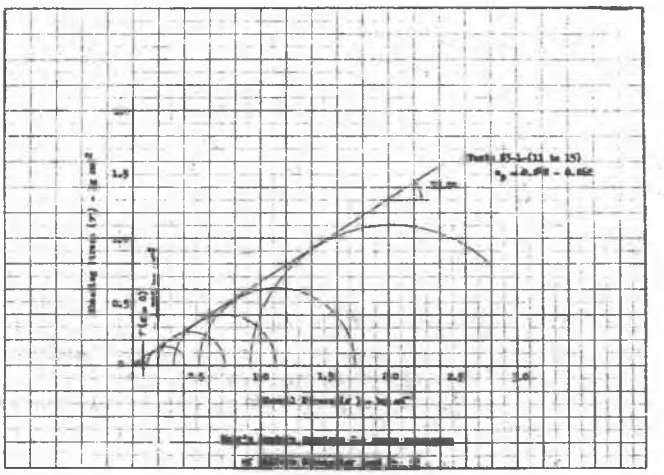

FIG.15

It is to be observed from Figs. 7-9 that a test specimen can be very accurately duplicated by following the procedures of placing and compacting soil as outlined previously.

STRESS-STRAIN AND STRENGTH CHARACTERISTICS OF COHESIONLESS SOILS AS FUNCTIONS OF DENSITY AND LATERAL PRESSURE.

A series of triaxial compression tests was conducted on subangular sand No. 83 (see Fig. 24) using five different densities ranging from the loosest to the densest states, and with lateral pressures ranging from 0.1 to 0.9 kg/sq cm.

Figs. 10-12 show the stress-strain curves for three of five states of density tested under different lateral pressures. In these and other figures, e_p stands for the void ratio of a test specimen at the start of loading $(\sigma_3)_o$ the lateral pressure at the start of loading $(\sigma_3)_f$ the lateral pressure corresponding to the maximum value of the ratio of axial to lateral stress. It is to be noted that the lateral pressure on a test specimen increased toward the end of the test because of a slight increase in the confining pressure exerted by the rubber tube as mentioned above.

Observation of Figs. 10-12 shows that for values of deviator stress within the range from

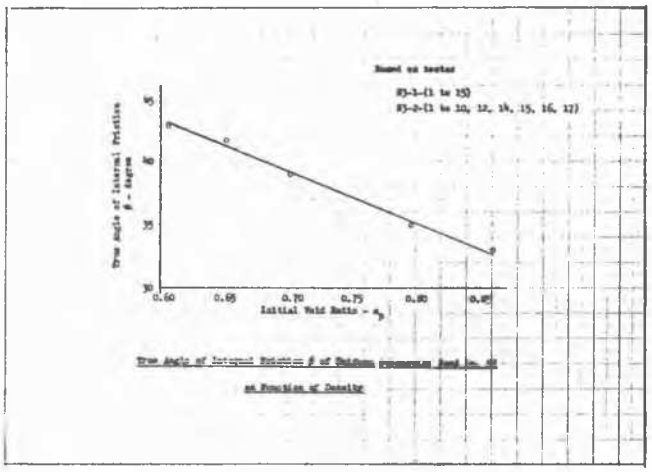

FIG.16

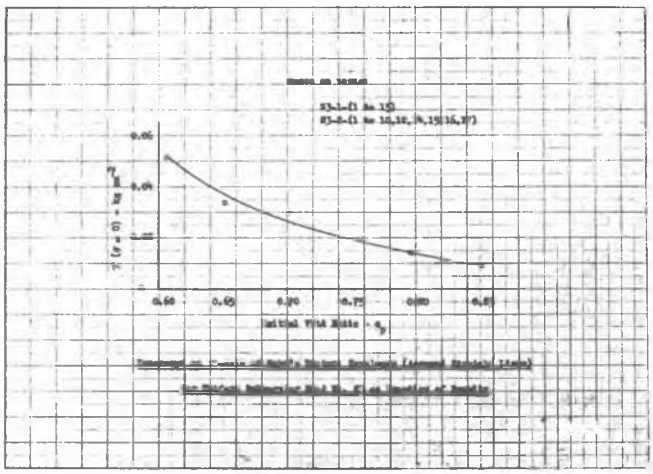

FIG.17

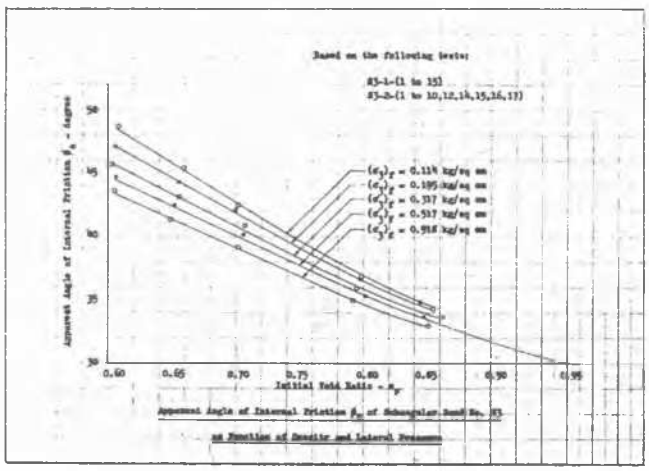

FIG.18

about 15% to 50% of the maximum deviator stress the stress-strain curves on logarithmic plots can be approximated closely by straight lines.

Figures 13-15 show the envelopes of Mohr's stress circles at failure. It is seen that these envelopes are approximately straight lines intersecting the τ-axis very slightly above the origin. The relationship between the slope (expressed by angle $\emptyset$, called the true

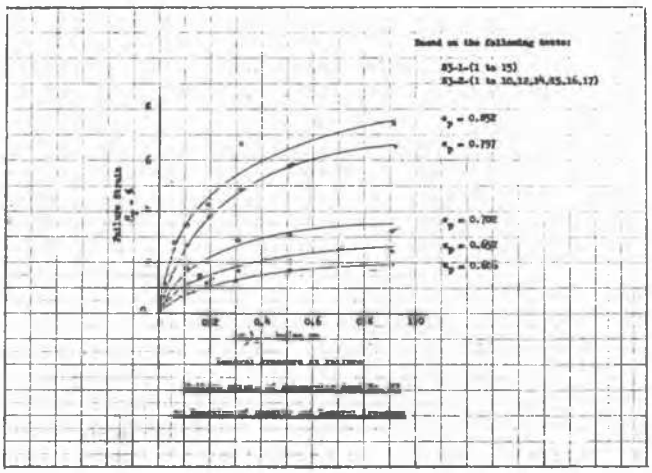

FIG.19

angle of internal friction) and the intersection on the τ-axis of the straight-line envelopes and the density of the specimens are shown in Figs. 16 and 17 respectively.

Owing to the fact that Mohr's rupture envelopes were not exactly straight lines passing through the origin, the angle $\emptyset_c$ between the σ-axis and the tangent from the origin to a failure stress circle, called the apparent angle of internal friction, was not a constant for a given density of soil, but decreased with increasing lateral pressure as shown in Fig.18.

As shown in Fig. 19, the failure strain ε_f, i.e. the axial strain corresponding to the maximum value of the ratio of axial to lateral stress, decreased with the density but increased with the lateral pressure.

RELATIONSHIP BETWEEN AXIAL AND LATERAL STRAINS

In Figs. 20 and 21 are shown the typical relationships between the lateral and axial strains of a dense specimen of subangular sand No. 81 (Fig. 24) and a loose specimen of Standard Ottawa sand. The lateral expansion of both test specimens was measured at the mid-height cross-section by means of four extensometers (Fig. 2). It is seen that equal increments of axial strain do not cause equal increments of lateral strain. For convenience, the ratio of a small increment of lateral strain to the corresponding small increment of axial strain will be called the tangent Poisson's ratio of soil. Observation of Figs. 20 and 21 shows that the tangent Poisson's ratio of sand subjected to a constant lateral pressure increases with increasing axial strain. For the dense and loose specimens, this ratio increased from a value smaller than 0.1 for small values of axial strain to about 1.6 and 0,8, respectively, at the failure strains.

The tangent Poisson's ratio also varies with the density of, and the lateral pressure on, test specimens, as illustrated in Figs.22 and 23. For a given axial strain, this ratio increases with increasing density and with decreasing lateral pressure.

Figure 22 shows that the volume of the loosest specimen at the failure strain was smaller than that at the start of the test. For specimens of other densities, the volume at the failure strain was larger than that at the start of the test. The dashed line in Fig. 22 was drawn based on the assumption that the lateral surface of a test specimen at the failure strain is symmetrical with respect to

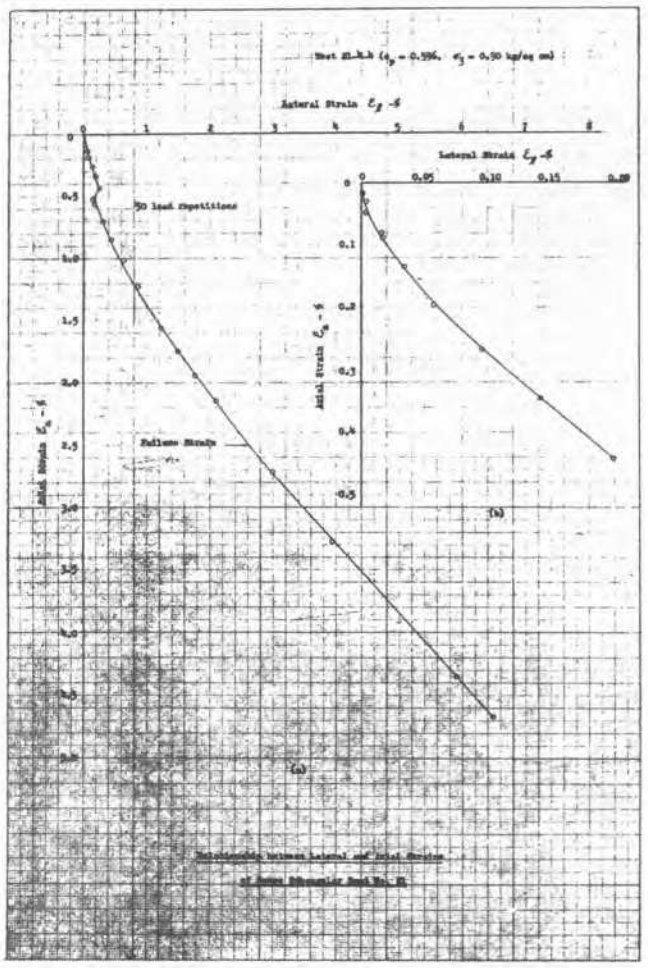

FIG. 20

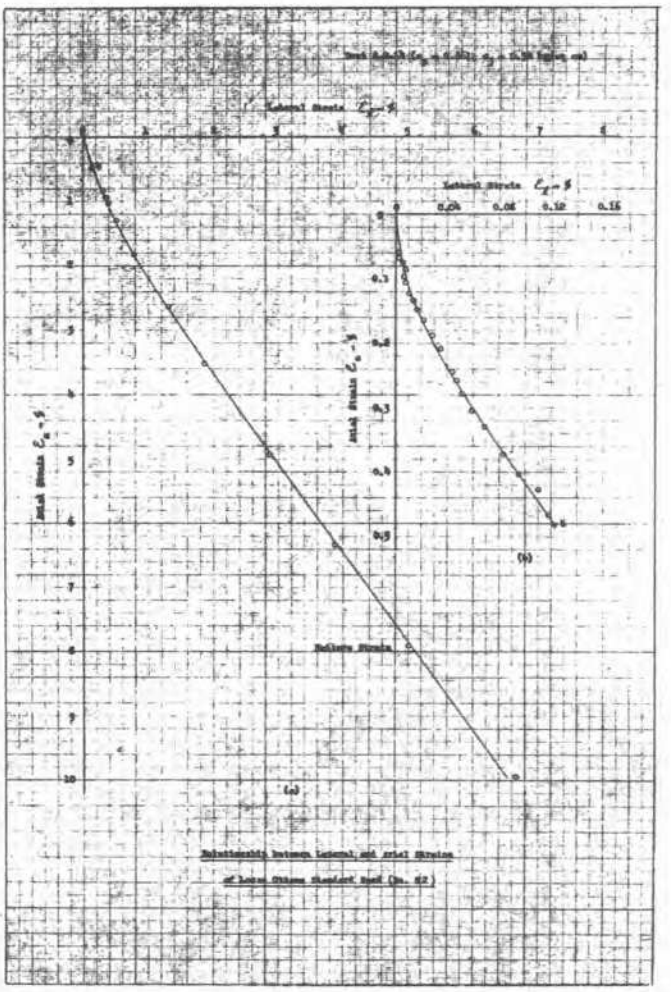

FIG. 21

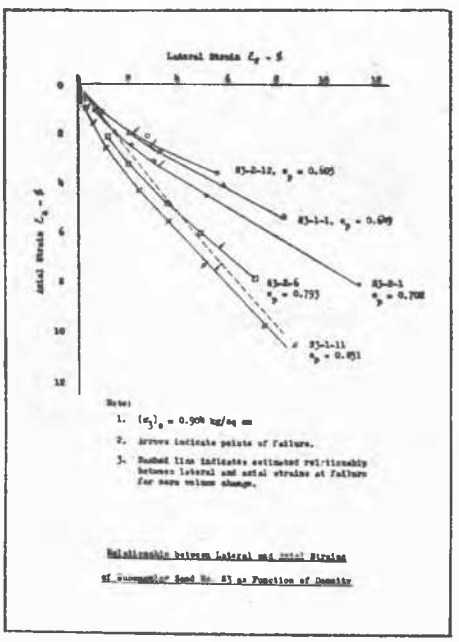

FIG.22

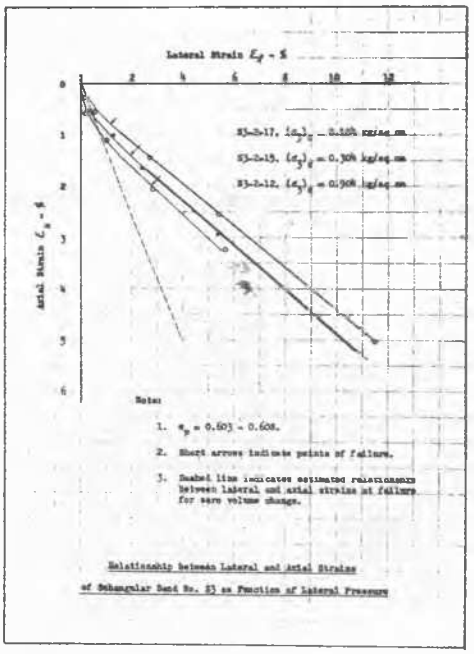

FIG. 23

the midheight cross-section and can be formed by revolving a section of a parabola about the axis of the specimen. This assumption was verified by a number of tests on subangelar sand S3.

STRESS-STRAIN AND STRENGTH CHARACTERISTICS OF COHESIONLESS SOILS AS FUNCTIONS OF ANGULARITY AND GRAIN-SIZE DISTRIBUTION.

Tests have been performed on a number of materials widely different in angularity and grain-size distribution (Fig. 24). Each material was tested at different densities ranging from loose to dense state, using a lateral pressure of 1.0 kg/sq cm. Each test was made by loading and unloading the test specimen twenty-five times to and from a deviator stress, $(\sigma_d)_r$, equal to about 30 percent of the estimated strength, before the specimen was finally recompressed to failure. The ratio of the repeated deviator stress $(\sigma_d)_r$ to the strain ε_{25} it produced along the last (25th) recompression curve was called modulus of compression and denoted by E_{25}.

Figures 25 and 26 show the apparent angle of internal friction ϕ_c and the modulus of compression E_{25}, respectively, of different materials as a function of density. It is seen that the apparent angle of internal friction ϕ_c increases with increasing angularity of grain and with increasing Hazen's coefficient of uniformity C_u (d_{60}/d_{10}), varying from 26.5° for loose specimens of the well-rounded Ottawa standard sand to 51.5° for the well-graded gravel. The modulus of compression E_{25}, however, decreases with increasing angularity of grain, and is not appreciably affected by the shape of the grain size distribution curves. That is, materials having angular grains are more compressible than materials having rounded grains, whereas the grain size has little effect on compressibility.

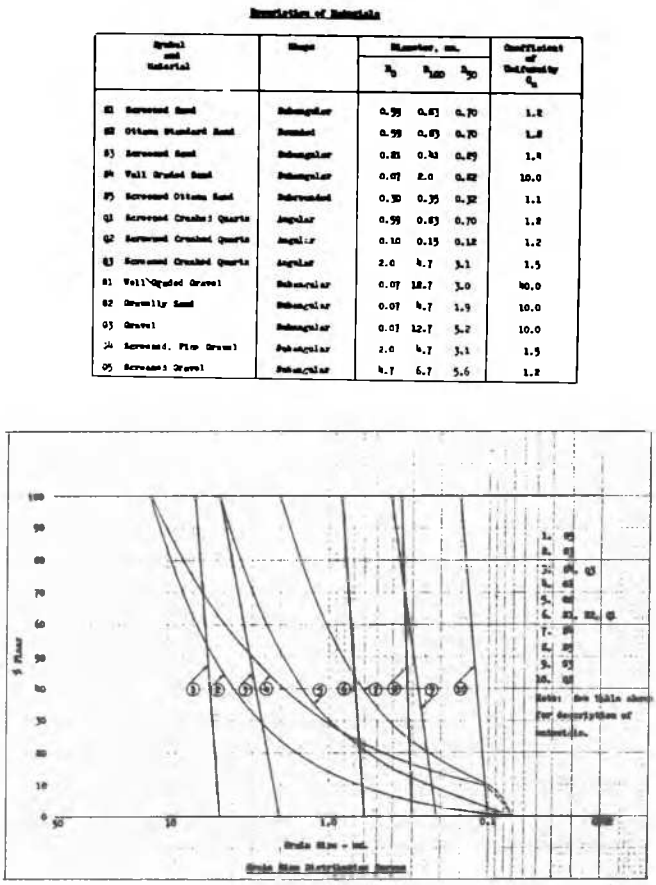

FIG. 24

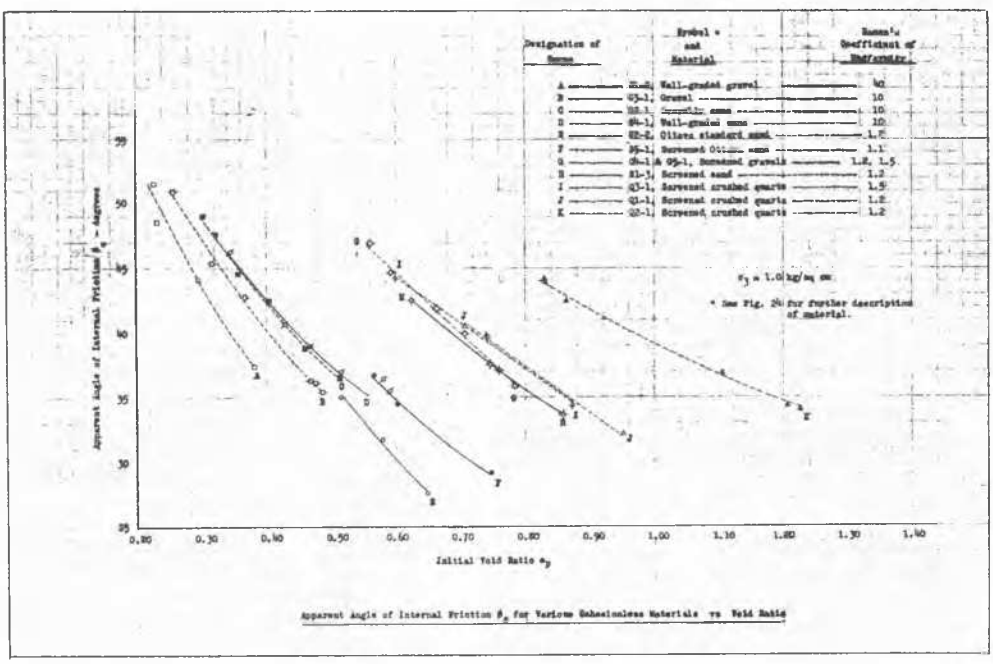

FIG. 25

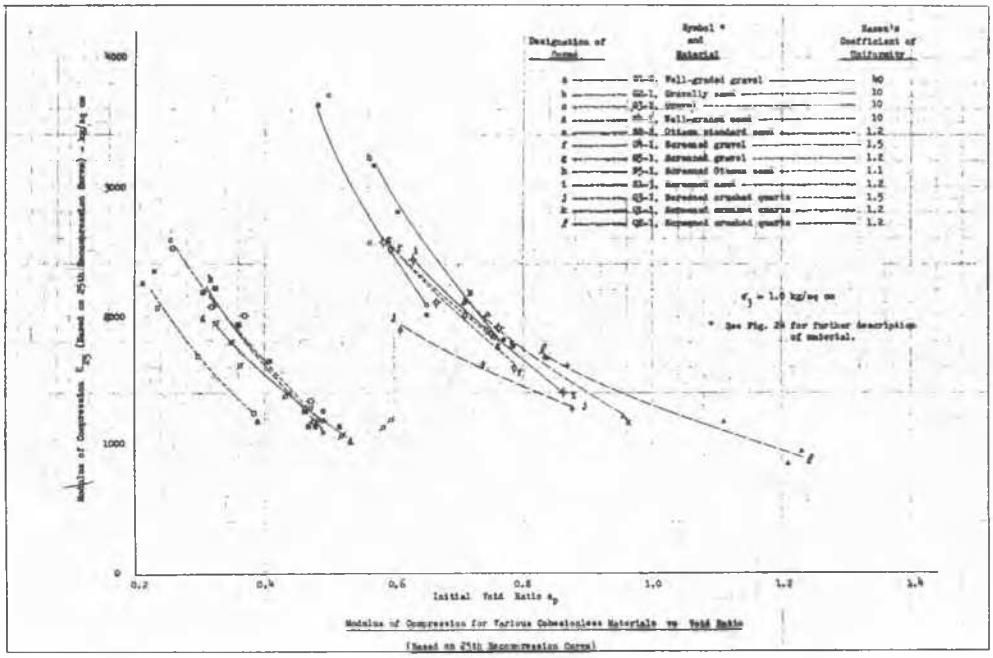

FIG. 26

CONCLUSIONS

The investigations presented above lead to the following conclusions:

1) The stress-strain and strength characteristics of cohesionless soils can be accurately determined by means of a simple vacuum type triaxial compression apparatus for the dry state and for confining pressures less than one atmosphere.
2) By means of improved equipment for placing and compacting cohesionless soils, great uniformity in the density of test specimens was achieved. It was also possible to duplicate accurately a given density and test results.
3) For the tests performed, the major portion of the stress-strain curves can be approximated by straight lines on logarithmic plots.
4) The angle of internal friction of cohesionless soils increases with increasing angularity of the grain and with increasing Hazen's coefficient of uniformity.
5) The compressibility of cohesionless soils increases with the angularity of grain, but is not appreciably affected by Hazen's coefficient of uniformity.
6) The lateral strain of test specimens of cohesionless soils increases at a faster rate than the axial strain. A cohesionless soil subjected to a constant lateral pressure does not possess a constant Poisson's ratio.

-o-o-o-o-o-o-

THE CAUSES OF THE JERKY PROCESS OF DEFORMATION IN THE CASE OF SATURATED AND DAMP SANDS

II d 12

WALTER BERNATZIK
Innsbruck, Austria

By subjecting sand-cylinders to pressure tests we find that in the case of dry sand, the process of deformation is steady, and parallel tests carried out by means of precisely working apparatus show practically no dispersion. On the other hand, tests with damp sands as well as with sands saturated with water, even if carried out with the greatest care, have shown that only the initial and final stages of the tests, i.e. the first stages of deformation and break load are free from dispersion. As soon as the process of deformation ceases to take a linear course and begins to develop progressively, deformation takes place by jerks and is accompanied by considerable dispersion which cannot be avoided even though tests be carried out with the greatest possible care and precision. The cause of this phenomenon is as follows: As long as the shearing forces from grain to grain are nowhere strong enough to surpass friction, deformation takes place practically without changing the density of the bedding and in linear manner. However, with an increased main tension ratio, a progressive displacement of grains takes place until the entire mass of sand is set in motion at break point. Displacement is accompanied at the beginning by a slight compression, which in its final stages develops into a loosening of the structure as shown by Figure No 1.

It will be seen that while the density of the bedding remains unchanged, two main tension